ELSEVIER

FEMS Microbiology Letters 188 (2000) 75–79

FEMS MICROBIOLOGY Letters

www.fems-microbiology.org

Three-dimensional modelling of the catalytic domain of *Streptococcus mutans* glucosyltransferase GtfB

Yau-Wei Tsai [a], Jean-Shan Chia [b], Yuh-Yuan Shiau [a], Hsiu-Chuan Chou [a], Yen-Chywan Liaw [c,1], Kuo-Long Lou [a,*]

[a] *Graduate Institute of Oral Biology, College of Medicine, National Taiwan University, No. 1, Chang-Teh Street, Taipei, Taiwan*
[b] *Graduate Institute of Microbiology, College of Medicine, National Taiwan University, No. 1, Chang-Teh Street, Taipei, Taiwan*
[c] *Institute of Molecular Biology, Academia Sinica, No. 128, Sec. 2, Yen-Chiou-Yuan Road, Taipei, Taiwan*

Received 31 March 2000; received in revised form 14 May 2000; accepted 16 May 2000

Abstract

Glucosyltransferases (GtfB/C/D) of *Streptococcus mutans*, a pathogen for human dental caries, synthesize water-insoluble glucan through the hydrolysis of sucrose. Genetic and biochemical approaches have identified several active sites of these enzymes, but no three-dimensional (3D) structural evidence is yet available to elucidate the subdomain arrangement and molecular mechanism of catalysis. Based on a combined sequence and secondary structure alignment against known crystal structures of segments from closely related proteins, we propose here the 3D model of an N-terminal domain essential for the sucrose binding and splitting in GtfB. A Tim-barrel of $(\alpha/\beta)_8$ structural characteristics is revealed and the structural correlation for two peptides is described.

Keywords: Glucosyltransferase; *Streptococcus mutans*; Sucrase activity; Catalytic domain; Three-dimensional model; Tim-barrel

1. Introduction

Glucosyltransferases (GTFs; EC 2.4.1.5) of mutans streptococci are enzymes responsible for the synthesis of water-soluble and -insoluble glucose polymers (glucan) from sucrose. These polysaccharides enhance the colonization of cariogenic bacteria and promote the formation of dental plaque on tooth surfaces [1]. Genetic approaches have identified several GTFs of distinct characteristics in oral streptococci including *Streptococcus mutans* (for review, see [2]). *S. mutans*, the most prevalent mutans streptococci isolated from human oral cavity [3], produces three GTFs [4–6]: GtfB (162 kDa) and GtfC (149 kDa) synthesize primarily insoluble glucan, whereas GtfD (155 kDa) synthesizes exclusively a water-soluble one. In addition, in vitro assays of adherence to glass surface suggest that GtfB and -C are more important than GtfD for bacterial attachment [7].

Studies of the structure and functional relationship of the GTFs from *S. mutans* and *Streptococcus sobrinus* have identified several important domains and specific amino acid residues involved in enzymatic activities for glucan binding, sucrose hydrolysis and glucan synthesis [2]. (i) A C-terminal glucan-binding domain (GBD) is composed of multiple homologous direct repeat segments, approximately 510 residues [8]. GBD was shown to be essential for glucan synthesis but not for sucrase activity [9]. (ii) An N-terminal catalytic domain of about 900 amino acids [2] is capable of binding and the hydrolysis of sucrose [10]. This region is highly conserved among GTFs and two active sites in this region have been reported based on biochemical and genetic analyses. The first active site of nine residues containing a catalytic aspartic acid was observed in the stabilized glucosyl–enzyme complex [10]. Site-directed mutagenesis confirmed the essential role of this Asp residue for sucrase activity in GTFs [11,12]. Primary sequence alignment revealed that this nanopeptide is highly conserved in the amylases and α-glucosidases [13]. A second active site identified by Funane et al. [14] and by our group [13] at almost the same time, consists of 19 amino acids (named Gtf-P1) adjacent to the nine-amino acid active site. Our recent mutagenesis studies confirmed

* Corresponding author. Tel.: +886 (2) 23123456; Fax: +886 (2) 23820785; E-mail: kllou@ha.mc.ntu.edu.tw

[1] Also corresponding author. Tel.: +886 (2) 27899199; Fax: +886 (2) 27826085; E-mail: mbycliaw@ccvax.sinica.edu.tw

0378-1097/00/$20.00
PII: S0378-1097(00)00213-5

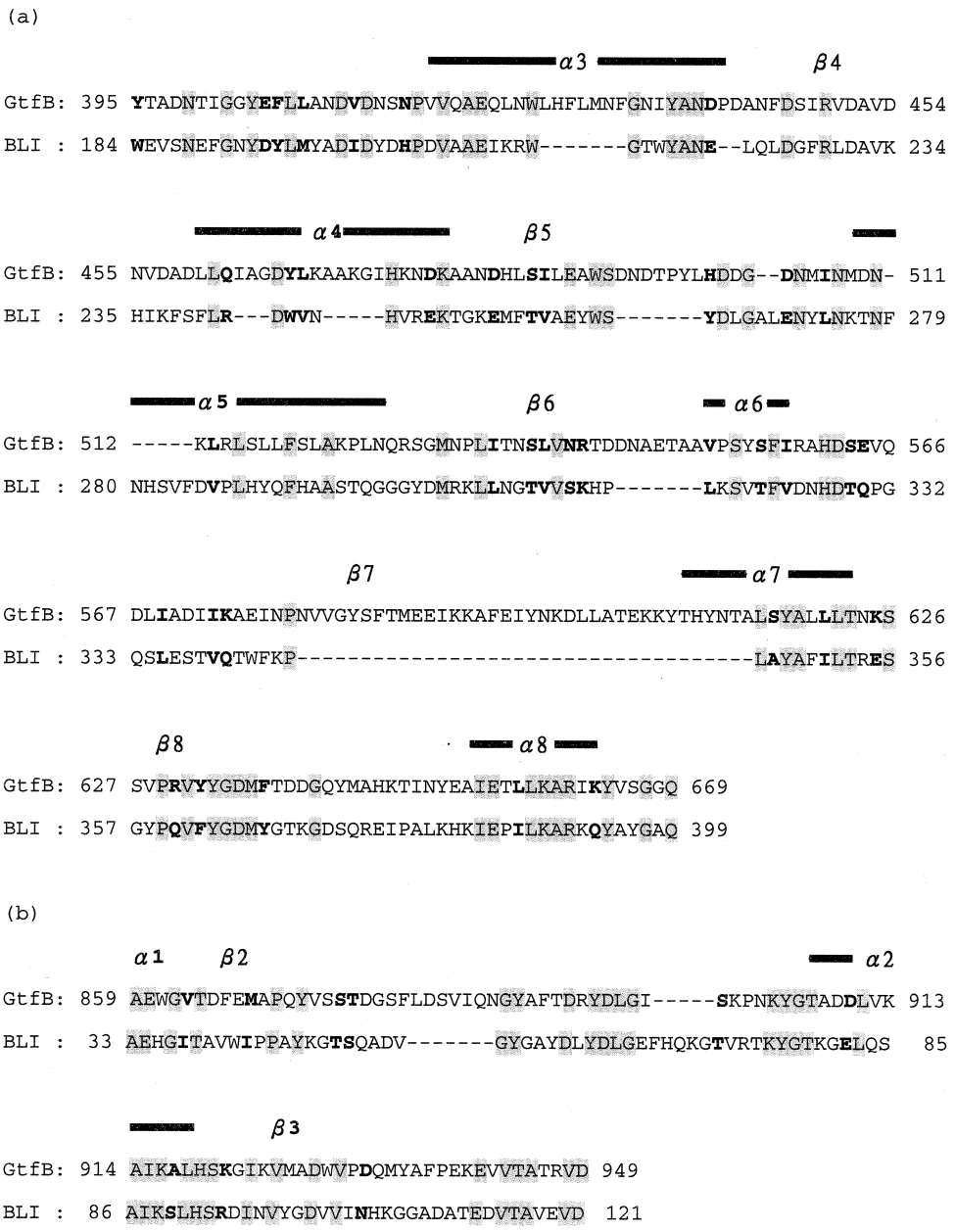

Fig. 1. Sequence alignment of GtfB [8] and BLI. Corresponding fragments for two proteins were chosen according to the results from paired sequence alignment. The residue identity for each fragment: (a) 21%, (b) 35%. Localization of α-helices and β-strands is marked on top of the residues according to their order in the GtfB structure. The shaded characters represent GtfB residues with high homology to template BLI. All amino acid residues are represented with single-letter abbreviations.

that two Asp residues in Gtf-P1 are essential for sucrase activity but may play different roles in GtfB and -C [15]. Taken together, the N-terminal one-third of the GTFs may play a central role in sucrose splitting and glucan synthesis. However, direct structural evidence indicating the subdomains and special residues responsible for these chemical details, as well as the molecular mechanism based on the conformational changes of these regions, remain to be determined. Therefore, based on a combined sequence and secondary structure alignment against the known crystal structure of segments from closely related proteins, we propose here the three-dimensional (3D) model of the catalytic domain of GtfB of *S. mutans*. The reason to start such work on GtfB is based on the results of mutagenesis and on the role of Gtf-P1 in various GTFs, which indicated that GtfB is more important in human cariogenesis and that Gtf-P1 may play a more crucial role in GtfB than in another GTF, GtfD [1,7,11,13].

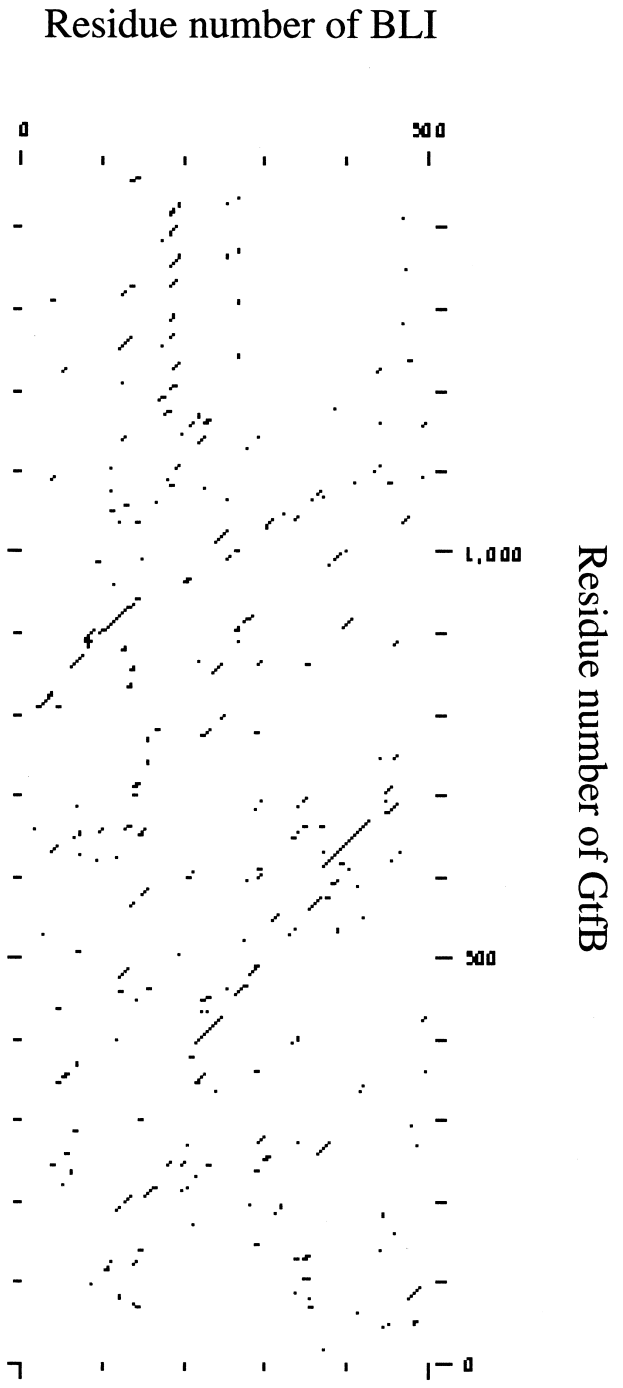

Fig. 2. Equivalent residues of GtfB and BLI determined by GCG programs. The plot shows the corresponding segments between GtfB and BLI. Each point represents an individual residue. The densely connected dot-lines indicate equivalent fragments with high homology between the two molecules. Note that the two dominant dense areas do not follow the order of their sequences.

2. Materials and methods

2.1. Search for templates

The BLAST algorithm was employed to search in PDB the protein segments whose sequences are similar to that of GtfB and whose structures can serve as viable structural templates. The crystal structures of three related amylases or glucosyltransferases (*Bacillus licheniformis* alpha-amylase, BLI [17]; alpha-amylase precursor, VJS [18]; glycosyltransferase, BPL [17]) which have shown the highest scores in the sequence alignments (BLI: 56; VJS: 55; BPL: 54) were chosen for the determination of structural conserved regions (SCRs). The GtfB residues used for model building are according to their paired sequence compared to BLI sequence. In addition, immediately after the primary sequence comparison with BLAST, part of the carboxyl- and amino-terminal residues of GtfB were eliminated according to the results.

2.2. Paired sequence alignment

The GCG program was used to determine the equivalent residues. Two residue regions of BLI represented as continuous lines dominantly observed in Fig. 2 were employed as appropriate template regions and the corresponding fragments in GtfB were chosen for alignment. The amino acid sequences of these GtfB fragments were then included in the multiple sequence alignment of the appropriate BLI regions to specify the residue numbers for model building [19].

2.3. Model building

Modelling by homology was performed essentially following the procedures described by Siezen [19]. Briefly, the two residue fragments of GtfB, 395–669 and 859–949 (from N- to C-termini), were chosen according to the results from paired sequence alignment. They were then superimposed onto the crystal coordinates of Cα atoms of the corresponding SCRs from BLI structure. This generated the secondary structure and relative position of the definite secondary structural elements in the two residue fragments of GtfB. Junctions between the secondary structural elements were individually regularized by energy minimization to give reasonable geometry. All the calculations and structure manipulations were performed with the Discover/Insight II molecular simulation and modelling programs (from Molecular Simulation Inc., San Diego, CA, USA; 950 release) on Silicon Graphics Octane/SSE workstation.

3. Results and discussion

3.1. Paired sequence and structural alignment

Sequence comparison and the residue identities between GtfB and BLI are shown in Fig. 1. The two residue fragments of GtfB used for structural alignment are residues 395–669 and 859–949 (from N- to C-termini), for which residues 184–399 and 33–121, respectively, of BLI are ap-

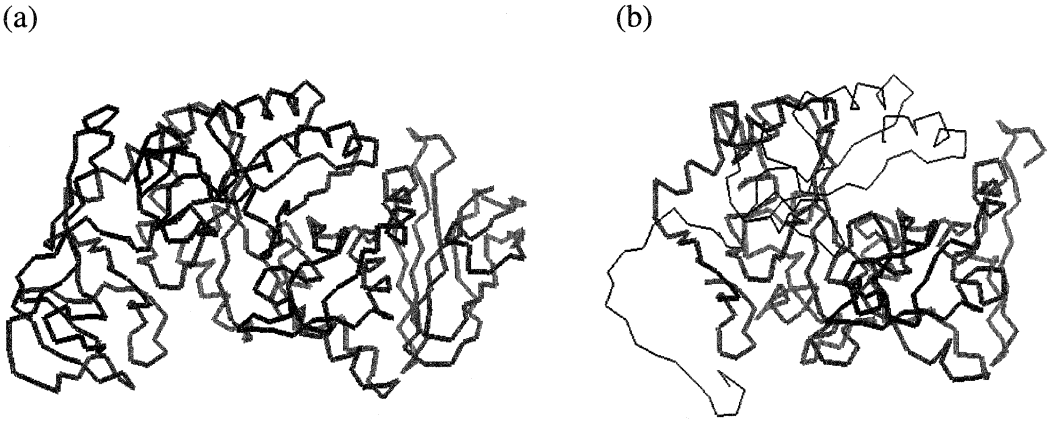

Fig. 3. Comparison of Cα-tracing between (a) BLI crystal structure and (b) GtfB model. In (b), lines with different thickness are used to distinguish the two parts of the molecule (see Section 3.1). Residues 395–669 are depicted with a broad line whereas residues 859–949 are with a fine line. Both diagrams are viewed with the barrel opening facing down. All drawings in this figure were made with Insight II software package.

plied to create coordinates (Figs. 1 and 2). It is interesting to note that regarding the best alignment available the corresponding fragments between GtfB and BLI are not in the order of their residue sequences (Fig. 2).

3.2. Overall structural features and comparison with template

Structural information from our model suggests the subdomain arrangement that coincides with the predictive structural arrangement for GTF-I from *Streptococcus downei* [16]. Such folding pattern of GtfB is also very similar to that of BLI [17] (Fig. 3). A typical Tim-barrel composed of eight consecutive units of α/β structural motif by forming the cavity for active sites, as observed in the crystal structures of other closely related sugar-splitting enzymes [17,18,20,21], was observed in this model (Figs. 3 and 4). The highly conserved 19-residue region, namely Gtf-P1 [13], spreads on the surface of the molecule in this model. It forms a fairly long α-helix and protrudes its N-terminal residues into the vicinity of the active site of the nine-residue fragment [10] (Fig. 4).

3.3. Substrate binding and sucrose splitting

The putative catalytic aspartate [10] is accessible by substrates from the wide opening of this cavity (Fig. 4). This may allow the sucrose to enter the specificity pocket and to bind to the enzyme molecule at the active site. According to the results from previous studies which suggested that the C-terminal one-third is responsible for the glucan binding [9], we would expect the long molecule of glucan to occupy the remaining part or outside of this cavity and to be supported by the C-terminal residues. However, due to the elimination of residues for structural alignment, almost all the one-third C-terminal residues of the molecule cannot be seen in this structure. Therefore, such an assumption remains to be verified.

We will not try to explain the chemical details of sucrose hydrolysis merely from this predictive model. However, based on the structural information and catalytic mechanisms obtained from crystal structures of other related amylases [17,18], a D-glucosyl–enzyme complex may be involve as an intermediate [2,10].

3.4. Monoclonal antibody recognition

One interesting structural interpretation provided by this model is the highly conserved 19-residue fragment, i.e. Gtf-P1 [13]. This peptide is located on the surface of the molecule in our model. Our previous results [22] have demonstrated that a monoclonal antibody against this region brought the sucrase activity of GtfB down to about

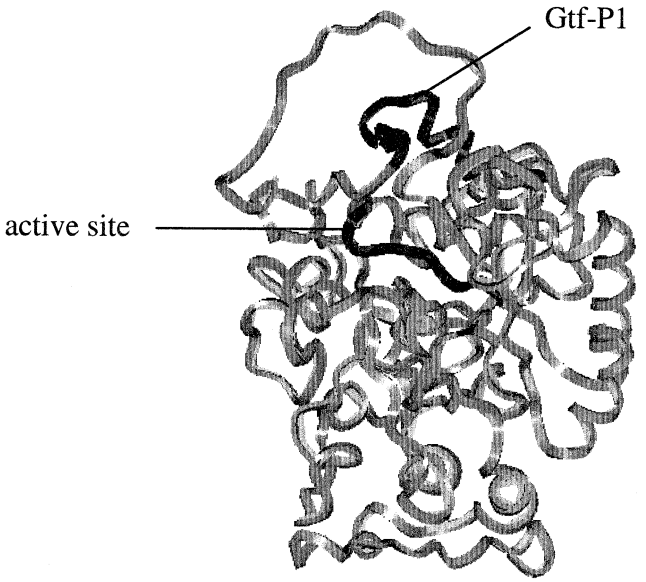

Fig. 4. Schematic diagram of the 3D model of GtfB with secondary structural elements. The figure is viewed from the opening of the catalytic pocket toward the active sites. Gtf-P1 and the nine-residue nanopeptide are marked in black to emphasize the location and structural correlation. All drawings in this figure were made with Insight II software package.

50%. Exposure of this 19-residue fragment on the surface of the molecule can lead to possible attack by an antibody. Conformational change of Gtf-P1 induced by such an attack may further affect the catalytic behavior via the protruding residues of this long α-helix into the vicinity of the active site (Fig. 4).

3.5. Conclusion

Our model has for the first time described 3D structural information for subdomain arrangement of the catalytic domain of GtfB and the structural correlation for two peptides required for enzyme catalysis. Due to the extraordinarily large size of the GtfB molecule, only structural properties with respect to the sucrase activity or catalytic domain could be deduced here from the currently available templates. Nevertheless, such information provides directions for further functional assays and the candidates for site-directed mutagenesis before the crystal structure of GtfB is determined.

Acknowledgements

The authors are very grateful to Dr. Ji-Wang Chern and Dr. Grace Shiahuy Chen at the Computer Modelling Center, NTUMC and Yi-Chun Tsai and Ting-Lin Chien from Hitron Technology Inc. for their enthousiastic discussion and for the possibility to use the Insight II programs. This work was supported in part by Grants 89-N4-CNB 88-03 (NTUMC R&D Committee) and NSC 89-2314-B-002-258 for K.L.L. and DOH88-HR-814 (NHRI) for J.S.C. We would also like to thank the financial support from Academia Sinica for Y.C.L.

References

[1] Hamada, S. and Slade, H.D. (1980) Biology, immunology, and cariogenicity of *Streptococcus mutans*. Microbiol. Rev. 44, 331–384.
[2] Monchois, V., Willemot, R.-M. and Monsan, P. (1999) Glucansucrases: mechanism of action and structure–function relationships. FEMS Microbiol. Rev. 23, 131–151.
[3] Loesche, W.J. (1986) Role of *Streptococcus mutans* in human dental decay. Microbiol. Rev. 50, 353–380.
[4] Honda, O., Kato, C. and Kuramitsu, H.K. (1990) Nucleotide sequence of the *Streptococcus mutans gtfD* gene encoding the glucosyltransferase-S enzyme. J. Gen. Microbiol. 136, 2099–2105.
[5] Shiroza, T., Ueda, S. and Kuramitsu, H.K. (1987) Sequence analysis of the *gtfB* gene from *Streptococcus mutans*. J. Bacteriol. 169, 4263–4270.
[6] Ueda, S., Shiroza, T. and Kuramitsu, H.K. (1988) Sequence analysis of the *gtfC* gene from *Streptococcus mutans* GS-5. Gene 69, 101–109.
[7] Fujiwara, T., Tamesada, M., Bian, Z., Kawabata, S., Kimura, S. and Hamada, S. (1996) Deletion and reintroduction of glucosyltransferase genes of *Streptococcus mutans* and role of their gene products in sucrose dependent cellular adherence. Microb. Pathol. 20, 225–233.
[8] Lis, M., Shiroza, T. and Kuramitsu, H.K. (1995) Role of C-terminal direct repeating units of the *Streptococcus mutans* glucosyltransferase-S in glucan binding. Appl. Environ. Microbiol. 61, 2040–2042.
[9] Nakano, Y.J. and Kuramitsu, H.K. (1992) Mechanism of *Streptococcus mutans* glucosyltransferases: hybrid-enzyme analysis. J. Bacteriol. 174, 5639–5646.
[10] Mooser, G., Hefta, S.A., Paxton, R.J., Shively, J.E. and Lee, T.D. (1991) Isolation and sequence of an active-site peptide containing a catalytic aspartic acid from two *Streptococcus sobrinus* alpha-glucosyltransferases. J. Biol. Chem. 266, 8916–8922.
[11] Kato, C., Nakano, Y., Lis, M. and Kuramitsu, H.K. (1992) Molecular genetic analysis of the catalytic site of *Streptococcus mutans* glucosyltransferases. Biochem. Biophys. Res. Commun. 189, 1184–1188.
[12] Devulapalle, K.S., Goodman, S.D., Gao, Q., Hemsley, A. and Mooser, G. (1997) Knowledge-base model of glucosyltransferase from the oral bacteria group of mutans streptococci. Prot. Sci. 6, 2489–2493.
[13] Chia, J.-S., Lin, S.-W., Yang, C.-S. and Chen, J.-Y. (1997) Antigenicity of a synthetic peptide from glucosyltransferases of *Streptococcus mutans* in humans. Infect. Immun. 65, 1126–1130.
[14] Funane, K., Shiraiwa, M., Hashimoto, K., Ichishima, E. and Kobayashi, M. (1993) An active-site peptide containing the second essential carboxyl group of dextransucrase from *Leuconostoc mesenteroides* by chemical modifications. Biochemistry 32, 13696–13702.
[15] Chia, J.-S., Yang, C.-S. and Chen, J.-Y. (1998) Functional analyses of a conserved region in glucosyltransferases of *Streptococcus mutans*. Infect. Immun. 66, 4797–4803.
[16] Monchois, V., Lakey, J.H. and Russell, R.R. (1999) Secondary structure of *Streptococcus downei* GTF-I glucansucrase. FEMS Microbiol. Lett. 177, 243–248.
[17] Machius, M., Wiegand, G. and Huber, R. (1995) Crystal structure of calcium-depleted *Bacillus licheniformis* alpha-amylase at 2.2 Å resolution. J. Mol. Biol. 246, 545–559.
[18] Hwang, K.Y., Song, H.K., Chang, C., Lee, J., Lee, S.Y., Kim, K.K., Choe, S., Sweet, R.M. and Suh, S.W. (1997) Crystal structure of thermostable alpha-amylase from *Bacillus licheniformis* refined at 1.7 Å resolution. Mol. Cells 7, 251–258.
[19] Siezen, R.J., Rollema, H.S., Kuipers, O.P. and de Vos, W.M. (1995) Homology modelling of the *Lactococcus lactis* leader peptidase NisP and its interaction with the precursor of the lantibiotic nisin. Prot. Eng. 8, 117–125.
[20] Jespersen, H.M., MacGregor, A.E., Henrissat, B., Sierk, M.R. and Svensson, B. (1993) Starch- and glycogen-debranching and branching enzymes: prediction of structural features of the catalytic (beta/alpha)$_8$-barrel domain and evolutionary relationship to other amylolytic enzymes. J. Prot. Chem. 12, 791–805.
[21] MacGregor, E.A., Jespersen, H.M. and Svensson, B. (1996) A circularly permuted alpha-amylase-type alpha/beta-barrel structure in glucan-synthesizing glucosyl-transferases. FEBS Lett. 378, 263–266.
[22] Chia, J.-S., Lin, R.-H., Lin, S.-W., Chen, J.-Y. and Yang, C.-S. (1993) Inhibition of glucosyltransferase activities of *Streptococcus mutans* by a monoclonal antibody to a subsequence peptide. Infect. Immun. 61, 4689–4695.